

# An introduction to the use of Sun-photometry for the atmospheric correction of airborne sensor data

**E. M. Rollin**  
**NERC EPFS**  
**Department of Geography**  
**University of Southampton**  
**Southampton, SO17 1BJ**

Contact: [emr@soton.ac.uk](mailto:emr@soton.ac.uk)  
Web site: [www.soton.ac.uk/~epfs](http://www.soton.ac.uk/~epfs)

---

## **Abstract**

Sun-photometry has a potentially important role to play in the atmospheric correction of airborne remotely sensed imagery. However, some understanding of the principles and limitations of Sun-photometry is vital to the successful utilisation of the technique for this purpose. This paper introduces the principles of Sun-photometry. It describes instrument characteristics, with particular reference to the EPFS Cimel CE 318-2. Sun-photometer measurements, the retrieval of atmospheric parameters and calibration issues are explained.

## **1. Introduction**

Sun-photometers are specialised narrow field-of-view radiometers designed to measure solar irradiance. They typically have between 6 and 10 well-defined spectral bands, each of the order of 10nm FWHM (Full Width Half Maximum). Modern instruments are electronically controlled, have on-board data storage capability and incorporate an automated tracking system for accurate positioning and pointing. Sun-photometer measurements can be used to recover atmospheric parameters, including spectral aerosol optical depth, precipitable water, sky radiance distributions and ozone amount. Aerosol volume and size distribution, are retrievable by inversion modelling from the spectral aerosol optical depth.

The atmospheric data retrievable from sun-photometers are primarily of use for meteorological and atmospheric applications (Schmid *et al.*, 1998), and this type of instrument has been used for many years by atmospheric scientists. However, the same data are also of potential value to remote sensing, especially for the atmospheric correction of remotely sensed imagery, and also in areas of field spectroscopy. In recognition of this, the NERC Equipment Pool for Field Spectroscopy has a CIMEL CE 318-2 portable sun-photometer (Figure 1) available for loan to support remote sensing projects. This paper focuses on the potential use for atmospheric correction of image data.

Atmospheric correction is essential for quantitative analysis of satellite and airborne remotely sensed imagery and the retrieval of surface biophysical information. It is especially important when absolute values of surface radiance are required or when small differences at the surface are superimposed on a large atmospheric component.

Where the atmospheric effect is modelled using radiative transfer codes, for example Lowtran 7 and 6S, aerosol parameters are required as input variables. These can be simulated from model atmosphere data, or generated from simultaneous ground data, including sun-photometers measurements. The *in-situ* approach offers a potential advantage because the values will be site and time specific and there is considerable evidence that the resulting atmospheric correction is more accurate than can be achieved by simpler methods (Chavez, 1996).

Despite the potential value to many remote sensing applications there is a scarcity of published work on the use of sun-photometer data for such applications and the remote sensing community remains largely unfamiliar with the principles of Sun photometry. The objective of this paper is to explain those principles for the benefit of the novice user. One over-riding point is that the sun-photometer does not measure atmospheric parameters directly, rather, these are retrieved from the measurements by a range of fairly standard data manipulations. However, instrument calibration and of the data manipulation will influence the retrieved parameters and impact on their accuracy. These influences are considered in the following review.



**Figure 1:** The EPFS CIMEL CE 318-2 Sun-photometer

## 2. Sun-photometers

Sun-photometers were first developed during the early part of the 20<sup>th</sup> century taking advantage of the new electrical thermopile devices and developments in the glass industry, which led to cut-off filters. These instruments were primarily designed to measure the solar constant using the spectral extinction method developed by S. P. Langley. This 'long method' is based on measurements of the solar flux in narrow wavelength bands at varying solar zenith angles and yields as a by-product the atmospheric transmissivity (Deirmendjian, 1980). The Voltz hand-held photometer, which was originally developed in 1959, includes two narrow spectral bands specifically for measuring atmospheric turbidity, and can be considered the precursor of modern sun-photometers.

Modern instruments vary little from early designs, but incorporate technological advances in optics and electronics and are generally more sensitive and much more stable. The basic sun-photometer design comprises a collimating tube defining a narrow angle (of the order of 1° to 3°), a series of interference filters and one (or more) solid state detector (usually, of the silicon photodiode type) with amplifier and a voltmeter. Two filter-detector arrangements are possible. In the filter-wheel arrangement, a series of filters is located on a rotating wheel and passed in turn in front of a single detector, resulting in sequential measurement of each band. Alternatively, in the multiple-detector arrangement each filter is fixed in front of a dedicated detector and all bands are measured simultaneously. Lenses may be present in the optical train, but are preferably avoided because they are unnecessary and their transmission properties can change when exposed to UV radiation. Most modern instruments incorporate microprocessor control of the measurement sequence, using Sun-seeking and Sun-tracking devices and zenith and azimuth stepping motors for accurate pointing and positioning to within 0.1°. They also include on-board data storage and/or data transmission capability. For positioning purposes, time must be known accurately and latitude and longitude must be input with high precision.

The filter characteristics are critical since these must define a narrow band-pass and be well-blocked (i.e. not allow the transmission of light outside the wavelengths limits of the band). Filters must also be well sealed in their mounts to prevent their exposure to pollutants and resulting deterioration. Modern instruments usually use thin film dielectric interference filters. Stability is fundamental to measurement accuracy and modern silicon photodiode detectors are well suited to the purpose. The need for portability means that power must be from batteries. Where instruments are deployed for automatic data collection, these can be recharged via solar panels. Wetness sensors, which detect precipitation and interrupt measurements accordingly, are essential for instruments operating in an automatic mode.

Figure 2 compares the extra-terrestrial solar spectral irradiance ( $E_0$ ) with a typical irradiance spectrum measured at the ground. The latter shows major absorption features due to atmospheric water vapour and oxygen which are not present in the extra-terrestrial spectrum. Recommended measurement wavelengths for retrieving information about various components of the atmosphere are also shown (based on those proposed by WRC/PMOD (Fröhlich, 1977)). However, sun-photometers differ considerably in their exact spectral specification in terms of number of bands and their

wavelength positions and bandwidths. Details of the CIMEL CE318-2 are summarised in Appendix 1.

Most sun-photometers are capable of measuring sky radiance. Variation in radiance in the circumsolar region, especially across the solar aureole (the area immediately adjacent to the solar disc), can be used to derive aerosol optical thickness, particle size distribution and phase function (Nakajima, 1983, Tanré *et al.*, 1988 and Shiobara, 1996).

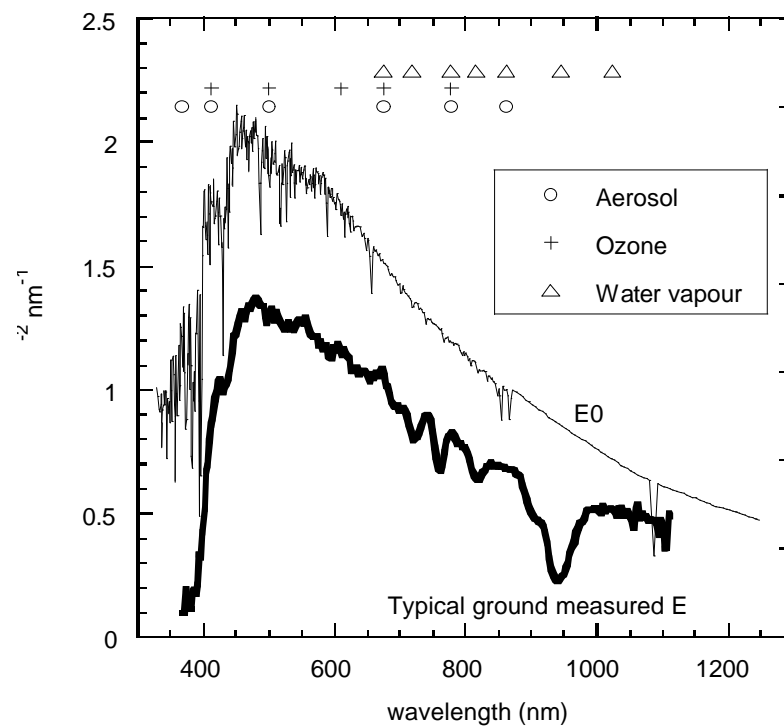


**Figure 2:** Extraterrestrial and ground measured irradiance with wavelengths for retrieval of atmospheric parameters superimposed

A relatively recent development has been the use of polarisation filters to measure the angular distribution and polarisation of sky radiance in order to extract aerosol size distribution information. However, the retrieval of atmospheric parameters from photopolarimetric measurements is more complex because it must take into account multiple scattering processes that affect sky radiance (Sano *et al.*, 1996).

### 3. Direct Sun Measurements

Direct solar beam measurements are obtained when the Sun collimator is trained on the solar disc. The detector output voltage for all wavelength channels is recorded and stored, together with the measurement time. Measurements are usually repeated at

frequent intervals, of the order of a minute separation or less. Data from each spectral band can be manipulated to quantify the atmospheric transmission, total and aerosol optical depth, and the amount of precipitable water (or water column abundance). These stages are explained in more detail in the subsequent sections. Figure 3 summarises the procedure schematically.

### 3.1 Atmospheric transmittance, total and aerosol optical depth and precipitable water

Transmission of the direct solar beam through a vertical slice of the atmosphere can be expressed as the voltage measured at the surface ( $V$ ) as a ratio of voltage expected at the top of the atmosphere, otherwise known as the calibration constant,  $V_0$ . This is not an exact radiometric calibration, but is the value the instrument would record outside the atmosphere, at an Earth-Sun distance of one Astronomical Unit (AU) and provides a band integrated value of the instrument response times the solar irradiance.

Atmospheric transmittance is a function of the attenuation of extra-terrestrial irradiance by scattering and absorption. When the direct beam is measured over a narrow band-pass (strictly, monochromatic radiation) the Beer-Lambert-Bouguer attenuation law holds and the instantaneous, total optical thickness for that wavelength ( $\tau_\lambda$ ) can be derived from:

$$V_\lambda = (V_{0\lambda}/R^2) \exp^{(-\tau_\lambda m)} \quad (1)$$

where,  $V_\lambda$  is the wavelength specific voltage,  $V_{0\lambda}$  is the calibration constant for that wavelength,  $R$  is the Earth-Sun distance in Astronomical Units at the time of observation of  $V_\lambda$ , and  $m$  is the relative optical airmass, which is approximated as the secant of the solar zenith angle (Kasten, 1965). An expression to compute the Earth-Sun distance,  $R$ , is given in Bird and Riordan, 1986. Rearranging and taking the logarithm of equation 1 leads to equation 2, which provides the basis for deriving both the  $V_{0\lambda}$  calibration constant by the Langley method (described further in section 4) and the optical depth:

$$\ln V_\lambda = \ln (V_{0\lambda}/R^2) - \tau_\lambda m \quad (2)$$

Provided  $\tau_\lambda$  remains constant over a series of measurements,  $V_{0\lambda}$  is determined as the ordinate intercept of a least squares fit of the plot of the left side of equation 2 against airmass,  $m$ , and  $\tau_\lambda$  is recovered as the slope of the line. Alternatively, if the  $V_{0\lambda}$  calibration of the instrument is already known, the instantaneous optical depth can be obtained from any individual measurement by:

$$\tau_{\lambda} = - \ln V_{\lambda} / (V_{0\lambda} / R^2) / m \quad (3)$$

The accuracy with which  $\tau_{\lambda}$  can be retrieved depends on the uncertainty of the  $V_{\lambda}$  measurement and the accuracy of the  $V_{0\lambda}$  value. Modern silicon photodiode detectors are very high precision, so the uncertainty in  $V_{\lambda}$  can be ignored. The accuracy of  $V_{0\lambda}$  is considered in section 4.

The total optical depth ( $\tau_{\lambda}$ ) is the result of attenuation by molecules (Rayleigh scattering), aerosols (Mie scattering, resulting from interaction of the radiation with larger particles), ozone, water vapour and other uniformly mixed gases. Each of these components can be separated. The Rayleigh component ( $\tau_{r\lambda}$ ) is readily calculated, depending only on the wavelength and barometric pressure at the surface (Hansen and Travis, 1974). Ozone has a variable but small effect which can be calculated based on tabulated values of the ozone absorption coefficient and assumptions about the ozone amount in Dobson units (e.g. Komhyr *et al.*, 1989). The effect of other mixed gases is constant but most sun-photometers use bands outside their influence, so their contribution can usually be ignored. This leaves aerosol and water vapour as the largest variable components and both of these may vary enormously in space and time.

The aerosol optical depth ( $\tau_{a\lambda}$ ) can be obtained by subtraction of the Rayleigh ( $\tau_{r\lambda}$ ) and ozone ( $\tau_{oz\lambda}$ ) components from the total optical depth:

$$\tau_{a\lambda} = \tau_{\lambda} - \tau_{oz\lambda} - \tau_{r\lambda} \quad (4)$$

Absorption by water vapour, is restricted to narrow spectral bands. The extraction of water vapour amount from sun-photometer measurements generally relies on a measurement in the region of water vapour absorption at 940nm. The aerosol effect is removed by extrapolating the value based on an adjacent band outside the absorption or, by interpolation between two adjacent bands. Equation 1 is not valid since exponential attenuation applies strictly to monochromatic radiation and is invalid across the broad region of water vapour absorption. Transmission in the water vapour band ( $T_w$ ) can be modelled as:

$$T_w = \exp(- a m^b W^b) \quad (5)$$

where  $W$  is vertical column abundance and constants  $a$  and  $b$  depend on the wavelength position, width and shape of the sun-photometer filter function, and the atmospheric conditions (temperature-pressure lapse and the vertical profile of water vapour band). Halthore *et al.*, (1997) showed that for a narrow (less than 10nm) band, sensitivity to the atmosphere can be removed and the following equation holds:

$$V_{\lambda} = (V_{0\lambda}/R^2) \exp(-m\tau) \exp(-aw^b) \quad (6)$$

where  $\tau$  is the Rayleigh plus aerosol optical depth, which are estimated independently (as described above) and  $w$  is the water column abundance (equal to the airmass,  $m$ , multiplied by the precipitable water (PW)). A modified Langley calibration is needed for the water vapour band (see section 4.1).

### 3.2 Spectral aerosol optical depth and aerosol particle size distributions

The variation in aerosol optical depth with wavelength, or the spectral aerosol optical depth ( $\tau_{a\lambda}$ ), defines the attenuation of solar irradiance as a function of wavelength and provides the basis for retrieving the columnar size distribution of the atmospheric aerosol. Figure 4 shows the spectral aerosol optical depth obtained from sun-photometer measurements at Southampton Common on 18/03/99. The relationship between the wavelength dependence of the spectral aerosol optical depth and the size of atmospheric aerosol particles was first suggested by Ångström (1929). Since then, a variety of numerical inversion methods have been developed to derive aerosol size distribution from spectral optical depth measurements (e.g. Yamamoto and Tanaka, 1969, King *et al.*, 1978). Some inversion algorithms superimpose the particle sizes based on a mathematical fit of the data (e.g. to Gaussian or Jungian distributions). Others derive the shape of the particle size distribution curve by an iterative procedure. Figure 5 shows the particle size calculated from the spectral aerosol optical depth data from Southampton Common shown in Figure 4.

These numerical inversions produce values of the columnar size distribution,  $dN/d(\log R)$ . These units are  $\text{cm}^{-2}$  for each particle sizes (defined in terms of particle radius, and assuming a spherical shape). To convert from the columnar size distribution to the number of particles per unit volume (i.e. per  $\text{cm}^{-3}$ ),  $dN/d(\log R)$  should be divided by the height of the column,  $H$ . This assumes the aerosol is uniformly distributed throughout the column, when in fact under normal conditions in the real atmosphere most of the aerosol is confined to the boundary layer, or lowest 2km of the atmosphere. Values of  $dN/d(\log R)$  can be converted to volume distributions ( $dV/d(\log R)$ ) which contains more information about the aerosol loading of the atmosphere, by multiplying by  $4/3\pi R^3$ , where  $R$  is the median radius of the size bin.

Limitations of the inversion procedure include the accuracy with which the measurement wavelength is known and the number and range of wavelengths over which  $\tau_{a\lambda}$  is measured (Amato *et al.*, 1995). King *et al.* (1978) point out that measurements must be made over sufficient wavelengths that the inversions are not affected by the sensitivity to the radii limits of maximum sensitivity and the refractive index values assumed in the inversions.

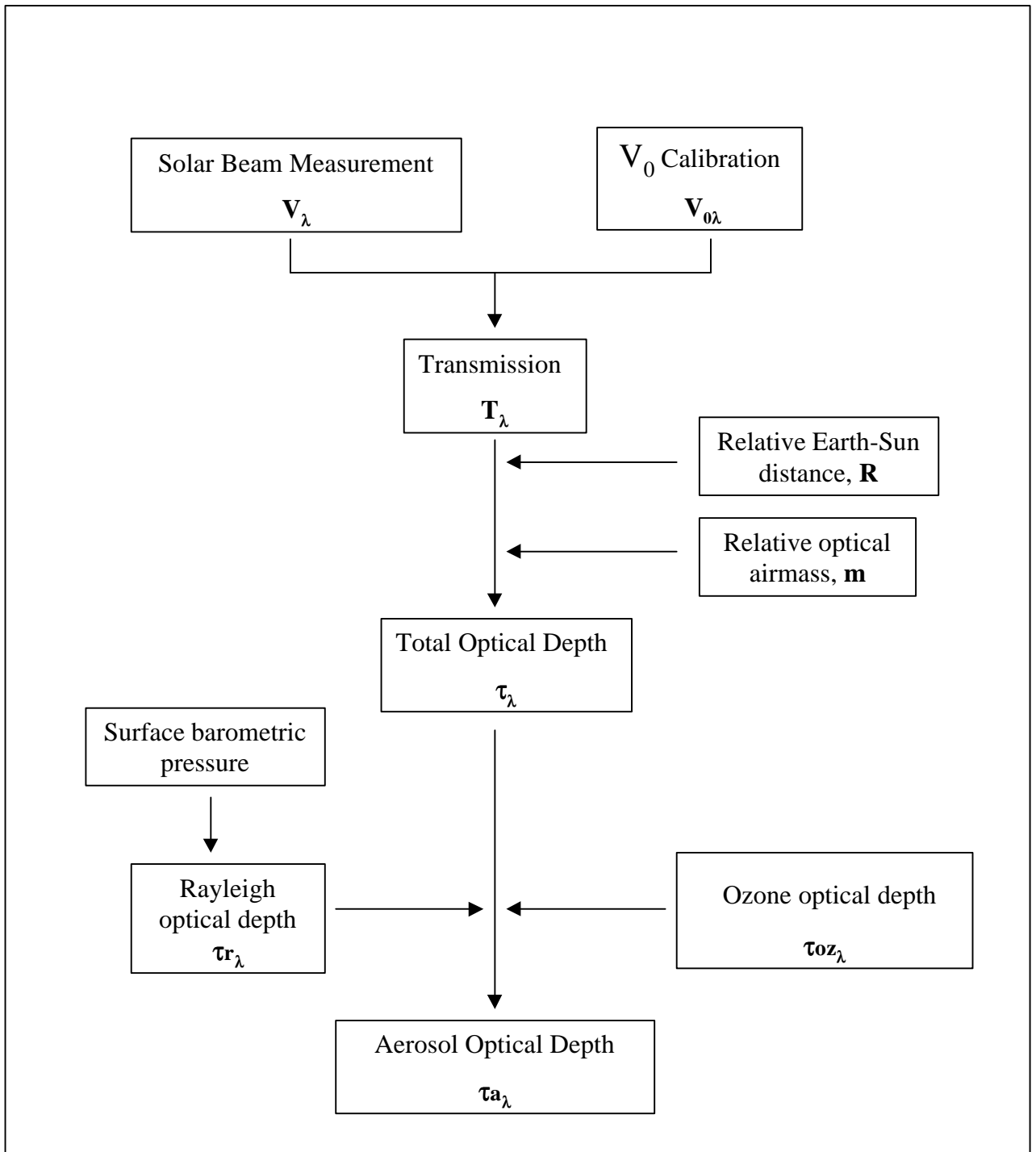


**Figure 3:** Schematic diagram of aerosol optical depth retrieval from direct beam measurements

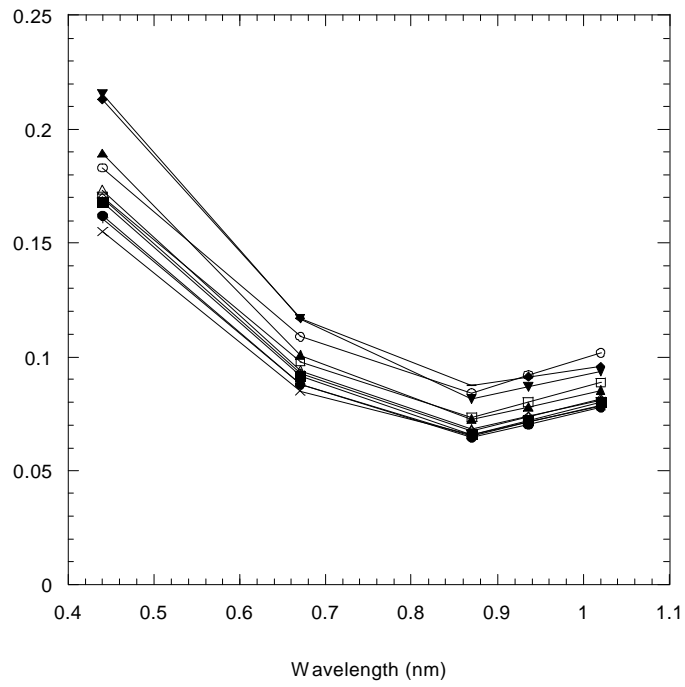


**Figure 4:** Aerosol Optical Depth Southampton Common (18/3/99)

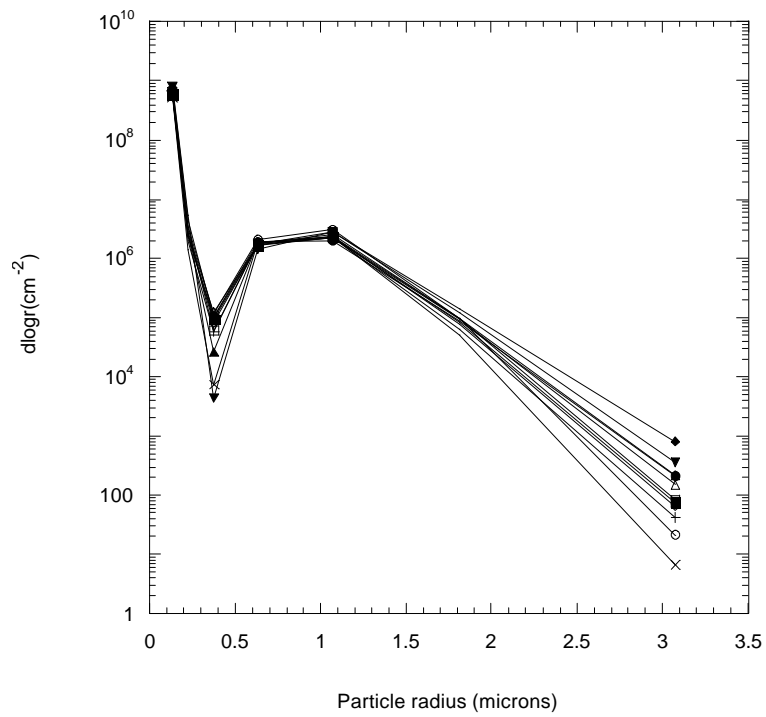


**Figure 5:** Particle size distribution Southampton Common (18/3/99)

## 4. Solar Aureole Measurements and Sky Radiance Profiles Measurements

The brightness of the solar aureole and its radiance gradient out to about  $6^\circ$  are dependent on the overall number of aerosol particles, and the size distribution. Under conditions of moderate turbidity the contrast between sky background and aureole brightness increases with wavelength (Deirmendjian, 1980). The aureole technique extracts aerosol optical thickness, particle size information and phase function using a relatively simple theoretical interpretation of predominantly single-scattering processes (Nakajima, 1983). The method is sensitive at low turbidity and is commonly used to complement direct beam measurements, which are more effective as turbidity increases. In order to retrieve aerosol parameters from the sky radiance measurements, the data must be calibrated to units of radiance ( $\text{W m}^{-2} \text{sr}^{-1} \text{nm}^{-1}$ ), (see section 5.2).

The Almuqantar and Principal Plane sky radiance profiles are standard sky measurement sequences that transect the region of the solar aureole. The Almuqantar profile (Figure 6) is in the horizontal plane at the solar zenith angle, with measurements at specified azimuths relative to the Sun through the full  $360^\circ$  of azimuth. Almuqantar measurements are typically made at an airmass of 2 or less to maintain large scattering angles. The Principal Plane (Figure 7) comprises a sweep of the sky in the vertical plane, rotating about an axis orthogonal to the solar azimuth, and spanning approximately  $150^\circ$ . The sequence usually starts with an observation of the Sun then moves to an angle below the Sun and sweeps the sky in the solar principal plane to an angle of  $140^\circ$  relative to the Sun. In the Principal Plane sequence each measurement angle relative to the Sun equals the scattering angle. In both observation sequences measurements are performed at a small angular interval in the region of the Sun (of the order of  $1^\circ$  to  $2^\circ$ ) and at a greater interval ( $10^\circ$  or more) away from it. The CIMEL CE 318-2, employs a second detector with larger entrance slit for the measurements of the sky beyond the solar aureole. Details of the Almuqantar and Principal Plane sequences for the CIMEL CE 318-2 are given in Appendix 2.

## 5. Calibration

Appropriate and accurate instrument calibration is required in order that absolute atmospheric parameters can be retrieved from sun-photometer measurements with an acceptable uncertainty. The most important calibration is the  $V_0$  calibration, but several others require consideration.

### 5.1 The $V_0$ calibration

For direct beam measurements in a particular wavelength band, the calibration constant of a sun-photometer ( $V_0$ ) is the value the instrument would record outside the atmosphere, at an Earth-Sun distance of one AU (Astronomical Unit), and provides a band integrated value of the instrument response times the solar irradiance. The Langley plot or Long plot method of field calibration is the preferred and most commonly used method of defining the  $V_0$  voltage.

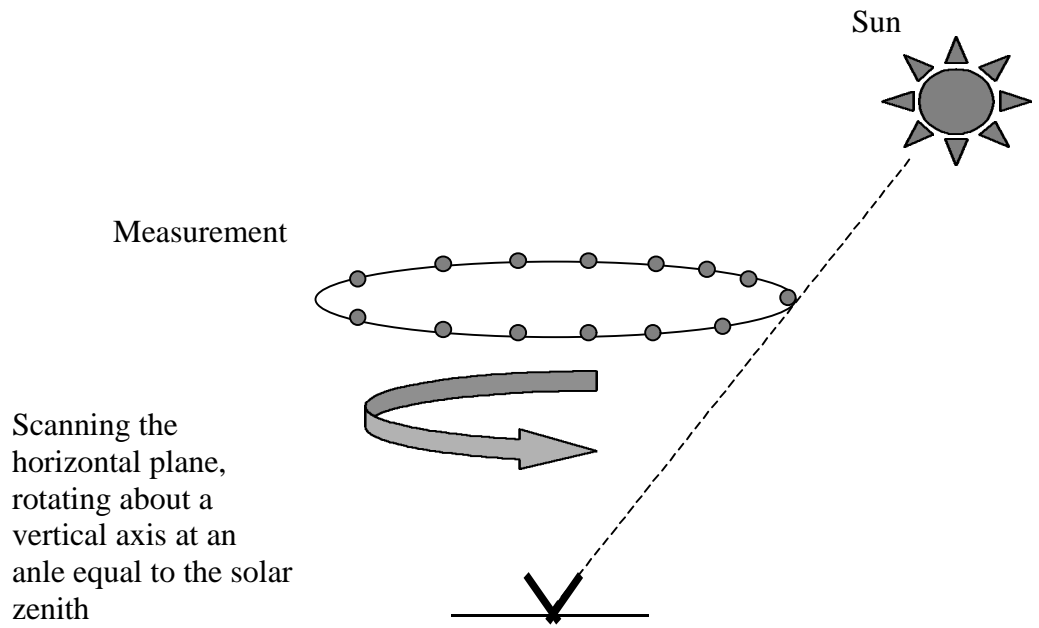


**Figure 6:** Almicantar Sky Radiance Profile

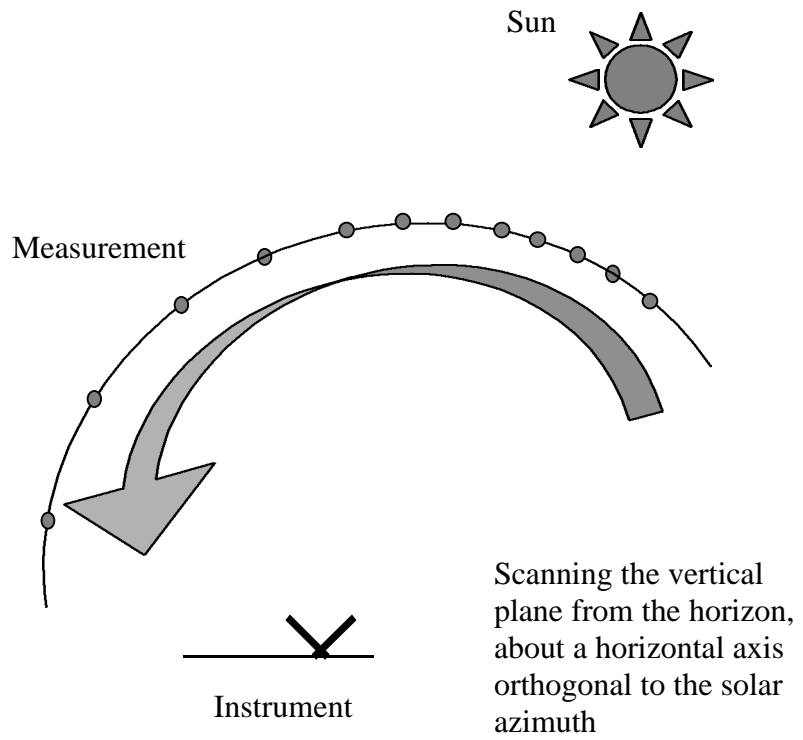


**Figure 7:** Principal Plane Sky Radiance Profile

i) The Langley method

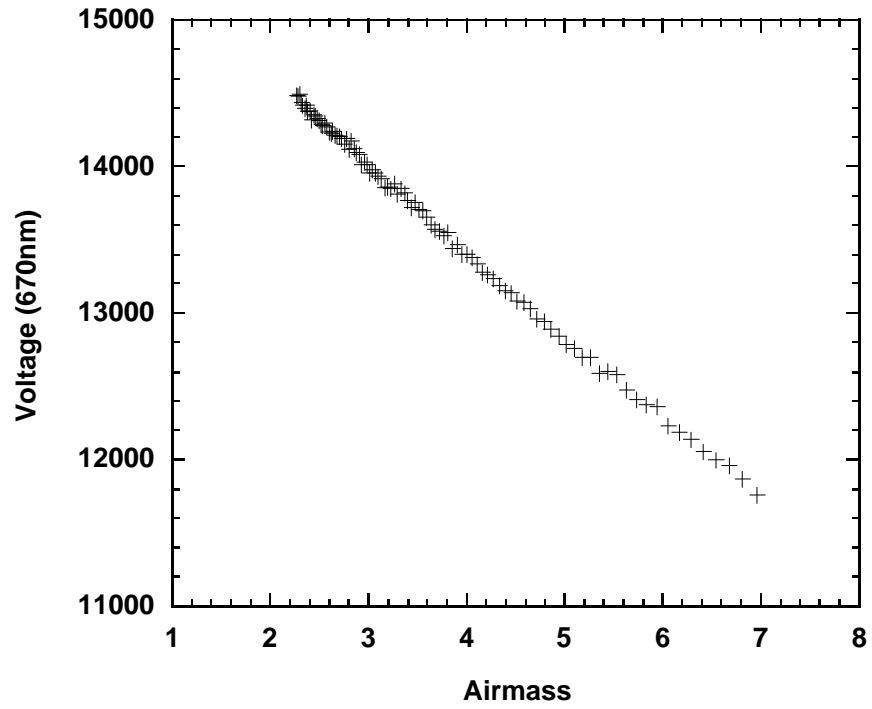
The Langley method is based on the principle of spectral extinction and relies on the Beer-Lambert-Bouguer Law. The extinction of the solar beam through different depths of atmosphere is measured and plotted and from this a value is extrapolated for a measurement at the top of the atmosphere. The procedure requires the instrument voltage for the direct solar beam to be measured at a number of different depths of atmosphere. In principle, the measurements should be obtained simultaneously at different elevations through the atmosphere. In practise, it is impossible to make the measurements simultaneously at different elevations with the same instrument, so the principle is applied by measuring the direct solar beam at one location over a range of solar elevation angles, providing measurements at different relative depths of atmosphere, or airmass (m). Solar elevation angle is related to airmass by the approximation  $\text{airmass (m)} = \sec \theta_z$ , (or  $m=1/\cos \theta_z$ ), where  $\theta_z$  is the solar zenith angle. Then, for each wavelength, a plot of the logarithm of the voltage against airmass yields  $V_{0\lambda}$  as the ordinate intercept (according to equation 2). When the Rayleigh ( $\tau_{r\lambda}$ ) and ozone ( $\tau_{oz\lambda}$ ) contributions are known, plotting the left side of the equation 7 against airmass (m) yields a straight-line provided  $\tau_{a\lambda}$  is constant throughout the measurement period.

$$\ln V + m\tau_{r\lambda} + m\tau_{oz\lambda} = \ln (V_{0\lambda}/R^2) - m\tau_{a\lambda} \quad (7)$$

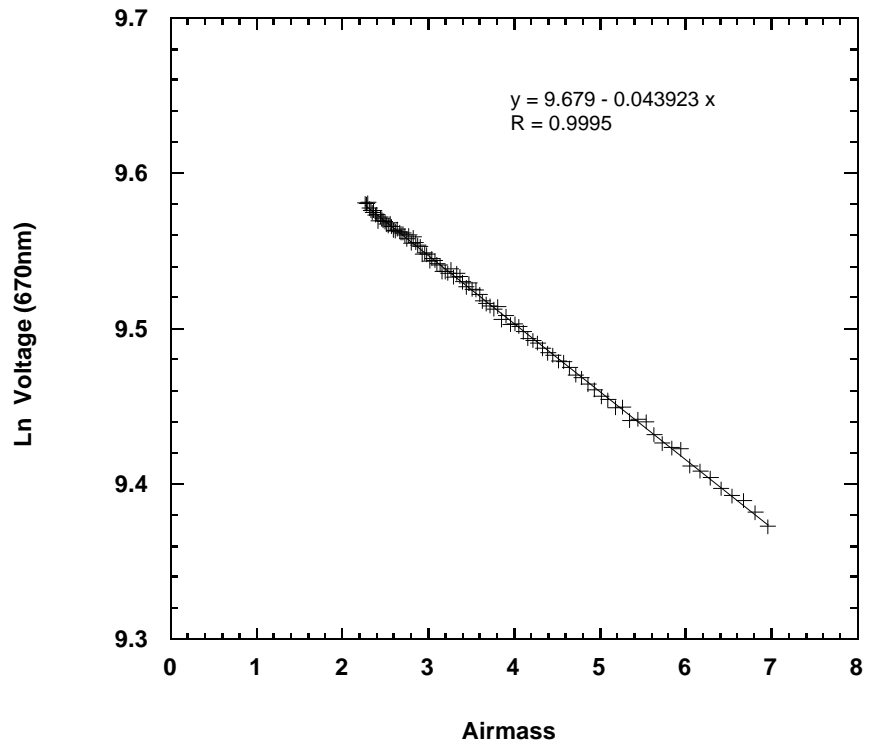
The intercept of a least-squares fit through the data provides the required calibration coefficient,  $V_0$  and the slope gives  $\tau_{a\lambda}$  for the measurement period. Measurements obtained over large zenith angles (between  $60^\circ$  and  $82^\circ$ ) covering the airmass range of 2 to 7, are essential for correct determination of the slope. Accurate determination of the Rayleigh and ozone components is critical for the Langley calibration. For the Rayleigh component, an accurate measurement of atmospheric pressure at the high altitude location is required.

Figure 8 shows the raw voltage measurements for the 670nm band of the EPFS CIMEL CE 318-2 obtained during a Langley calibration series obtained on Mt. Etna during July 1999. Figure 9 plots the as  $\ln(\text{voltage})$ . Adjustment of the raw voltages to subtract the Rayleigh and ozone contributions must be made before the correct intercept can be used to derive the  $V_0$  calibration.

The critical assumption of such Langley measurements is that the aerosol optical extinction remains constant throughout the period of measurement. This requires the atmosphere to be temporally invariant during the several hours required for the measurement sequence to be obtained, and horizontally homogeneous over a distance of about 50km. The latter requirement is because the measurements at different solar elevation angles traverse the surrounding atmosphere. Both assumptions are only likely to be valid at high-altitude locations (Schmid and Wehrli, 1995), where the aerosol component in any case is small. Low altitude and continental locations are more likely to be affected by temporal changes in atmospheric transmission over the time scale involved and are not generally suitable for performing Langley calibration. Forgan, (1994) claims that the Langley method is not an absolute method when used



**Figure 8:** Langley calibration series – Voltage against airmass (670nm)



**Figure 9:** Langley calibration series – Ln(voltage) against airmass (670nm)

in the troposphere and has a large uncertainty. Instead, he proposed a general method of calibration, which is essentially a modification of the Langley method but relaxes the constraints on atmospheric conditions

Because modern sun-photometers can obtain direct sun measurements at a high frequency (at the order of 1 or 2 seconds),  $V_0$  can be established with high precision. However, the accuracy of the  $V_0$  values obtained by the method is the subject of much attention, affected as it is by the measurement circumstances and in particular, any change in the atmosphere. Reagan *et al.*, (1984) cites the accuracy of  $V_0$  values from Langley plot as being typically between 4% and 10%. Shaw (1983) illustrates the danger of introducing systematic errors to Langley calibrations as a result of time-dependent changes in atmospheric transmission. To avoid this, he recommends that even calibrations performed at ideal, high altitude sites should be based on morning measurements only (before inversion layers breakdown due to solar heating and convection), and should be accompanied by simultaneous measurement of the aerosol directly, to confirm no changes in atmospheric transmission occurred. It is generally accepted that if the  $V_0$  values can be repeated on several days of independent measurement, they can be regarded as reliable (Shiobara *et al.*, 1996).

There are numerous variations and refinements of the Langley method, including those developed to allow more accurate removal of the non-aerosol components or to cope with sub-optimal data series (e.g. Soufflet *et al.*, 1992.). The method of Tanaka *et al.*, (1986) incorporates measurements of the solar aureole into the  $V_0$  calibration. Forgan (1994) formulated a general method of calibration based on the Langley method, but with more relaxed constraints on the atmospheric conditions.

A modified-Langley method is used for deriving calibration values for the water absorption band around 940nm (Bruegge *et al.*, 1992). The method requires the product of the precipitable water (PW) and airmass ( $m$ ), to be accounted for in addition to Rayleigh and ozone optical depth. In this case, the aerosol optical depth ( $\tau_a$ ) is estimated by interpolation between the two neighbouring channels. The modified Langley calibration for this band then becomes:

$$\ln V + m\tau = \ln (V_0/R^2) - aPW^b m^b \quad (8)$$

A plot of the left side of equation against  $m^b$  yields a straight-line with the ordinate intercept equal to  $\ln(V_0)$  and the slope equal to  $aPW^b$ .

## ii) Alternative $V_0$ calibration methods

In principle,  $V_0$  values can be derived from absolute radiometric calibration of the instrument in the laboratory then extrapolation of the calibration to the extraterrestrial solar irradiance spectrum (e.g. the tabulated values of Neckel and Labs, 1983). Laboratory calibration involves measuring against a calibrated irradiance source such as a high intensity tungsten lamp, and requires that the relative spectral response of the sun-photometer be known. Schmid and Wehrli, (1995) performed a comparison of

a laboratory calibration procedure with the Langley plot method and found reasonable accuracy for both and good agreement between the resulting  $V_0$  values, although they did report their results were sensitive to the extraterrestrial solar irradiance spectrum used. They concluded that laboratory techniques could and should be used to supplement regular field calibrations. Other workers consider that laboratory calibration cannot replace the Langley method (e.g. Shaw, 1980). Problems associated with laboratory calibration include the accuracy of the calibration of the source and its intensity, which may be several orders of magnitude lower than that of the Sun, and the need to overfill the detector field-of-view. The accuracy of this calibration will also depend on accurate spectral characterisation of the instrument bands (see 5.3).

Another method of effecting an absolute calibration is to cross-calibrate against a second, accurately calibrated instrument either in the field or against a laboratory source. Two considerations are important in this approach. Firstly, that differences between the instruments being inter-calibrated must be properly accounted for, especially their spectral band characteristics (bandwidth and relative spectral response). Secondly, calibration errors will be increased via inter-calibration and can be readily propagated across a network of instruments.

It is worth noting that all these methods require accurate information about the relative spectral response of the sun-photometer in all spectral bands, something not required for the Langley calibration method.

## 5.2 Radiance calibration of sky measurements

A laboratory procedure is normally used to determine the calibration coefficients needed to convert sky measurements from digital counts to units of radiance ( $\text{W m}^{-2} \text{sr}^{-1} \text{nm}^{-1}$ ). In this case, measurements are performed against a calibrated spectral radiance source (integrating sphere or irradiated reference panel). The calibration coefficient is then derived as:

$$L_\lambda / \text{DN}_\lambda \quad (9)$$

where  $L_\lambda$  is the radiance of the calibration source integrated over the spectral response function of the wavelength band and  $\text{DN}_\lambda$  is the measured response for that wavelength band. The accuracy of this calibration depends partly on the accurate spectral characterisation of the instrument bands, as described in the following section.

## 5.3 Other calibration considerations

### i) Spectral characteristics

All the relationships between the sun-photometer measurements and the retrieved parameters are wavelength sensitive and it is critical that the spectral characteristics of any particular instrument be accurately known. Ideally, the relative spectral response function for each band is required, but at minimum the wavelength of peak sensitivity and bandwidth (normally the full width at half maximum - FWHM) should be known. These characteristics should be established initially and also checked intermittently so

that any changes can be identified. Checks should certainly be carried out when changes in the sensitivity of the instrument are indicated since this may indicate filter deterioration, which is not uncommon.

ii) Temperature sensitivity

Solid state optical detectors are often temperature dependent and ideally should be thermostatically controlled. One method instrument manufacturers use to achieve a constant operating temperature is to provide heat to raise the operating temperature above ambient. Other manufacturers consider temperature control to be impractical for such a field instrument, preferring to record temperature and offer correction factors as necessary (these will normally be required for the longer wavelength bands). In this case it is important that operators are aware of any temperature dependent effects and make the necessary corrections.

iii) Temporal stability

Sensitivity variations of up to 10% over a year or less have been reported for some sun-photometers (Forgan, 1994). This underlines the importance of monitoring sensitivity as frequently as possible, with a combination of field techniques and laboratory calibration checks, something emphasised by several workers (e.g. Shaw, 1983), Forgan (1994) and Schmid and Wehrli, 1995). Data from the EPFS CIMEL show a fairly typical variation with time (Figure 10), and illustrate the difficulty of maintaining accurate  $V_0$  of the sun-photometer. In this case, the  $V_0$  for the bands centred at 660nm, 880nm and 1020nm changed by between 3% and 7% between 1997 and 1999. For the water vapour band at 940nm the change was greater (9.5%) although this may be due to a difference in boundary layer conditions between the two measurement dates. Data for the 440nm band indicate an apparent increase in sensitivity with a higher  $V_0$  value for the 1999 calibration than for that obtained in 1997. One possible cause of this would be a change in the efficiency of the filter between the two measurement dates, and this is currently under further investigation.

## 6. Data Processing Considerations

Modern sun-photometers operating in automatic mode can generate large volumes of data, which necessitates comprehensive methods for handling, processing and archiving the data. Despite this need, even commercially available instruments are often supplied without any dedicated support software. Software and data procedures have developed in a rather *ad hoc* way, possibly because of variation between instruments and the fact that many are unique, built for a particular location and objective. One important consideration for data collected in an automatic mode is the need to filter out cloud affected before processing.

From the users' perspective, it is important to recognise the enormous scope for variation in the implementation of the retrieval algorithms and inversion procedures, and the consequent effect of this on the results obtained. Algorithms can incorporate unique refinements and modifications and, in the numerical inversion modelling, assumptions about input parameters (such as the definition of aerosol particle shape and refractive index) are a particular source of uncertainty, which can affect the reliability of the atmospheric data retrieved. Similarly, the accuracy of the instrument

calibration coefficients and instrument spectral characterisation will also affect the results obtained.

Greatest effort to standardise the data processing algorithms and minimise the impact of calibration uncertainties has been made where similar instruments are operated as a network. AERONET (**A**erosol **R**obotic **N**etwork), operated by NASA is perhaps the largest network of sun-photometers, with instruments based world-wide (Holben *et al.*, 1998). This operates by transmitting raw data from the sun-photometers via the Data Collection System (DCS) using the GOES-E, GOES-W or METEOSAT satellites. Data are then filtered, calibrated and processed and can be accessed in near real-time via the Internet. A smaller network operates in Canada (AEROCAN). In Switzerland, the Swiss Atmospheric Radiation Monitoring Network, (CHARM) is a joint venture between three SWISS organisations and aims to make best use of the Swiss Alps for the purpose of radiation monitoring (Heimo *et al.*, 1998). Similar networks are under consideration elsewhere in Europe. One advantage of such networks provides opportunity for improved standardisation in aspects of sun-photometer calibration, algorithm implementation and data handling.

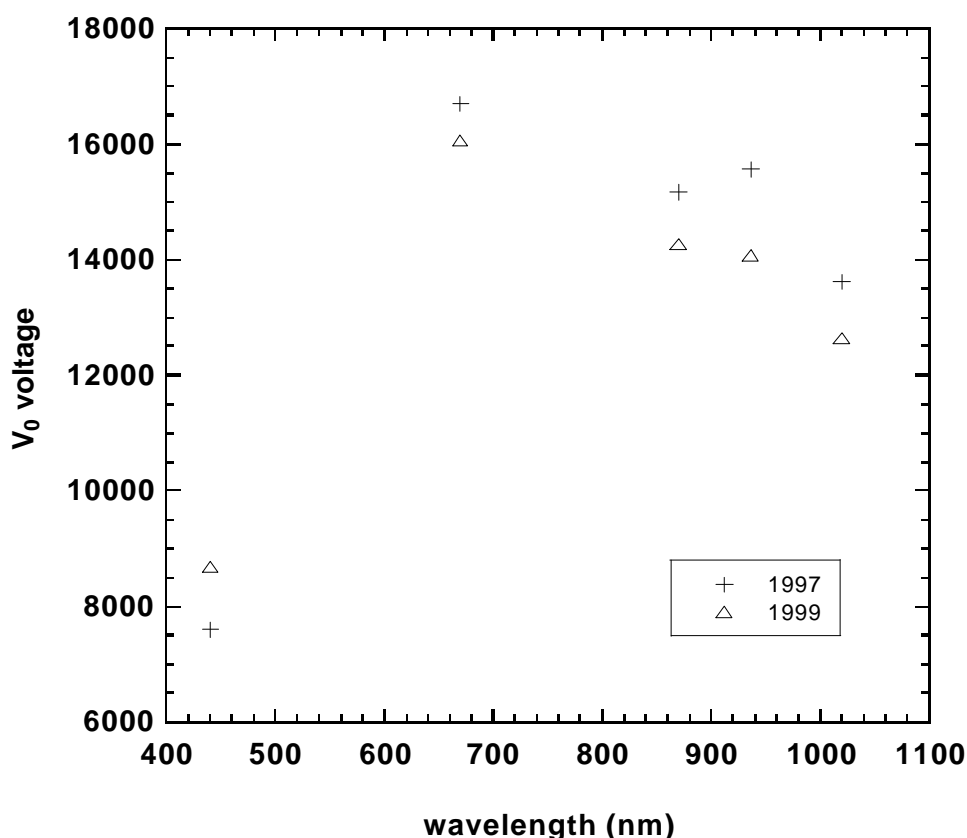


**Figure 10:** Comparison of  $V_{0\tilde{\epsilon}}$  calibration values for the EPFS CIMEL CE318-2 from 1997 (+) and 1999 (Δ).

## 7. Overview

The successful utilisation of sun-photometer derived atmospheric data to remote sensing applications requires an understanding of how those data are derived and some perspective on their limitations and quality. The following considerations are particularly important:

- i) the instrument configuration, characterisation and calibration,
- ii) data processing, including the filtering of sub-optimal data (e.g. cloud affected), the implementation of the algorithms and accuracy with which the non-aerosol components of optical depth are determined, inversion modelling with the associated assumptions.

The suitability of sun-photometer data for a specific task will also depend on other factors. For example, the advantage of sun-photometer derived data being time and location specific and therefore especially valuable for atmospheric correction of simultaneously acquired imagery may be compromised by the synoptic situation. Solar beam measurements with a sun-photometer traverse the slice of atmosphere between the instrument and the Sun. In most cases, this will be an oblique, rather than a vertical, slice through the atmosphere. For example at latitude of 50° N, even the noon solar zenith angle never falls below approximately 27°. The spatial extent over which the derived parameters will be representative will vary with conditions.

This review has focused on the principles of Sun-photometry with the aim of enlightening users away from the 'black-box' concept of the sun-photometer a source of absolute and error free atmospheric parameters. Understanding the principles and potential limitations of the technique are essential to the successful utilisation of Sun-photometry for atmospheric correction of remotely sensed imagery.

## References

- Amato, U., Esposito, F., Serio, C., Pavese, G. and Romano, F., 1995, Inverting high spectral resolution aerosol optical depth to determine the size distribution of atmospheric aerosol. *Aerosol Science and Technology*, 23, 591-602.
- Ångström, A., 1929, On the atmospheric transmission of sun radiation and on dust in the air. *Geografis Annal.*, 2,156-166.
- Bird, R.E., and Riordan, C., 1986, Simple solar spectral model for direct and diffuse irradiance on horizontal and tilted planes of the Earth's surface for cloudless atmospheres. *J. Clim. Appl. Meteorol.* 25, 87-97.
- Bruegge, C.T., Conel, J.E., Green, R.O., Margolis, J.S., Holm, R.G., and Toon, G., 1992, Water vapor column abundance retrievals during FIFE. *Journal Geophysical Research* 97:18759-18768.
- Chavez, P.S. Jr., 1996, Image-based Atmospheric corrections – revisited and improved. *Photogrammetric Engineering and Remote Sensing*, 62,1025-1036.

- Deirmendjian, D., 1980, A survey of light-scattering techniques used in remote monitoring of atmospheric aerosols. *Reviews of Geophysics and Space Physics*, 18, 341-360.
- Forgan, B. W., 1994, General method for calibrating Sun photometers, *Applied Optics*, 33, 4841-4850.
- Fröhlich, C., 1977, WRC/PMOD Sunphotometer: instructions for manufacture, World Meteorological Organisation Report, Geneva, Switzerland.
- Halothore, R. N., Eck, T. F., Holben, B. N. and Markham, B.L., 1997, Sun photometric measurements of atmospheric water vapor column abundance in the 940-nm band. *Journal of Geophysical Research*, 102, 4343-4352.
- Hansen, J. E. and Travis, L. D., 1974, Light scattering in planetary atmospheres, *Space Science Reviews* 16, 527-610.
- Heimo, A., Philipona, R., Fröhlich, C., Marty, Ch., and Ohmura, A., 1998, The Swiss Atmospheric Radiation Monitoring Network CHARM. *Proceedings of the World Meteorological Organisation Technical Conference on Meteorological and Environmental Instruments*, Casablanca, Morocco, May13-15 1998, WMO/TD-877:291-294.
- Holben, B. N., Eck, T. F., Slutsker, I., Tanre, D., Buis, J. P., Setzer, A., Vermote, E., Reagan, J. A., Kaufman, Y. A., Nakajima, t., Lavenu, F., Jankowiak, I. And Smirnov, A., 1998, AERONET – A federated instrument network and data archive for aerosol characterisation, *Remote Sensing of Environment*, 66:1-16.
- Kasten, F, 1965, A new table and approximation formula for the relative optical airmass. *Arch. Meteor. Geophys. Bioklim.*, B14 206-223.
- King, M. D., Byrne, D. M., Herman, B. M. and Reagan, J. A., 1978, Aerosol size distributions obtained by inversion of spectral optical depth measurements. *Journal of the Atmospheric Sciences*, 35, 2153-2167.
- Komhyr et al., 1989, Dobson Spectrometer 83: A standard for total ozone measurements, 1962-1987, *Journal of Geophysical Research*, 94, 9847-9861
- Nakajima, T., Tanaka, M. And Yamauchi, T., 1983, Retrieval of the optical properties of aerosols from aureole and extinction data. *Applied Optics*, 22, 2952-2959.
- Neckel, H. And Labs, D., 1983, The solar radiation between 3300 and 12500 Å. *Solar Physics*, 90, 205-258.
- Reagan, J. A., Scott-Fleming, I. C., Herman, B. M. and Schotland, R. M., 1984, Recovery of spectral optical depth and zero-airmass solar spectral irradiance under conditions of temporally varying optical depth, *Proceedings of IGARSS'84 Symposium*, Strasbourg, ESA SP-215, 455-459.

- Sano, I., Mukai, S., Takashima, T. And Yamaguchi, Y., 1996, Retrieval algorithms for photopolarimetric properties of aerosols. *Advances in Space Research*, 17, 163-166.
- Schmid, B. and Wehrli, C., 1995, Comparison of Sun photometer calibration by use of the Langley technique and the standard lamp. *Applied Optics*, 34, 4501-4512.
- Shaw, G. E., 1983, Sun Photometry. *Bulletin of American Meteorological Society*, 64, 4-10.
- Shiobara, M., Spinhirne, J. D., Uchiyama, A., and Asano, S., 1991, Optical depth measurements of aerosol, cloud and water vapour using sun photometers during the FIRE Cirrus IFO II. *Journal of Applied Meteorology*, 35, 36-46.
- Soufflet, V., Devaux, C. and Tanré, D., 1992. A modified Langley plot method for measuring the spectral aerosol optical thickness and its daily variations. *Applied Optics*, 31, 2154-2162.
- Tanaka, M., Nakajima, T., and Shiobara, M., 1986, Calibration of a sunphotometer by simultaneous measurements of direct-solar and circumsolar radiation, *Applied Optics*, 25, 1170-1176.
- Tanré, D., Devaux, C., Herman, M. and Santer, R., 1988, Radiative properties of desert aerosols by optical ground-based measurements at solar wavelengths. *Journal of Geophysical Research*, 93, 14223-14231.
- Yamamoto, G. and Tanaka, M., 1969, Determination of aerosol size distribution from spectral attenuation measurements. *Applied Optics*, 8, 447-453.

## Appendix 1 Summary of CIMEL CE 318-2

The CIMEL CE 318-2 spectral radiometer is manufactured by CIMEL Electronique of Paris, France. The instrument comprises:

- i) a robot
- ii) a sensor head with two 33 cm collimators, and
- ii) a logic box.

This sensor head incorporates two silicon detectors for measurement of the Sun, aureole and sky radiance. Both collimators have approximately a 1.2° full angle field of view and are designed for 10<sup>-5</sup> stray-light rejection for measurements of the aureole 3° from the Sun. The Sun collimator is protected by a quartz window allowing observation with a UV enhanced silicon detector with sufficient signal-to-noise for spectral observations between 300 and 1020 nm. The sky collimator a larger aperture-lens system for better dynamic range of the sky radiance. Eight ion assisted deposition interference filters are located in a filter wheel, which is rotated by a direct drive stepping motor.

The EPFS CIMEL CE318-2 is a polarised instrument, with 8 channels in total, three of which are polarised at 870nm. The centre wavelengths and FWHM (in brackets) are as follows:

- 440nm (10nm)
- 670nm (10nm)
- 870nm (10nm) – 1 x unfiltered channel, plus 3 x polarised channels
- 940nm (10nm)
- 1020nm (10nm)

The sensor head is pointed by stepping azimuth and zenith motors with a precision of 0.05 degrees. A microprocessor computes the position of the sun based on time, latitude and longitude which directs the sensor head to within approximately one degree of the sun, after which a four quadrant detector tracks the sun precisely

The robot and sensor head are sealed from moisture and desiccated to prevent damage to the electrical components and interference filters. A thermistor measures the temperature of the detector allowing compensation for any temperature dependence.

A solar panel provides power to the robot. When idle, the robot mounted sensor head is parked pointed vertically down. A "wet sensor" exposed to precipitation will cancel any measurement sequence in progress.

## **Appendix 2 CIMEL CE 318–2 Sky Radiance Profiles**

### **ALMUCANTAR**

Measurement angles (in degrees) relative to solar azimuth:

*0*, -6, -5, -4, -3.5, -3, -2.5, -2, 2, 2.5, 3, 3.5, 4, 5, 6, 6, 7, 8, 10, 12, 14, 16, 18, 20, 25, 30, 35, 40, 45, 50, 60, 70, 80, 90, 100, 120, 140, 160, 180, 200, 220, 240, 260, 270, 280, 290, 300, 310, 315, 320, 325, 330, 335, 340, 342, 344, 346, 348, 350, 352, 353, 354, 354, 355, 356, 356.5, 357, 357.5, 358, 366, 362, 362.5, 363, 363.5, 364, 365, 366

Sequence repeated for each wavelength band in order 1020nm, 870nm, 670nm, 440nm.

Italics indicate measurement with Sun collimator. Other measurements are with sky collimator.

### **PRINCIPAL PLANE**

Measurement angles (in degrees) relative to Sun zenith:

*0*, -6, -5, -4, -3.5, -3, -2.5, -2, 0, 2, 2.5, 3, 3.5, 4, 5, 6, 6, 8, 10, 12, 14, 16, 20, 25, 30, 35, 40, 45, 50, 55, 60, 65, 70, 80, 90, 100, 110, 120, 130, 140, 150

Italics indicate measurement with Sun collimator. Other measurements are with sky collimator.

Negatives indicate angles below the Sun.

Sequence repeated for each wavelength band in order 1020nm, 870nm, 670nm, 440nm.